RAPID COMMUNICATIONS

PHYSICAL REVIEW B VOLUME 32, NUMBER 10 15 NOVEMBER 1985

Angle-resolved photoelectron spectra using realistic surface potentials: Evidence for surface-induced structure in TiC(001)

J. Redinger and P. Weinberger
Institute für Technische Elektrochemie, Technische Universität Wien, A-1060 Vienna, Austria

E. Wimmer
Cray Research, Mendota Heights, Minnesota 55120

A. Neckel
Institut für Physikalische Chemie, Universität Wien, A-1090 Vienna, Austria

A. J. Freeman
Department of Physics, Northwestern University, Evanston, Illinois 60201
(Received 21 August 1985)

Angle-resolved photoemission spectra for TiC(100) are calculated using Pendry's method and realistic surface potentials obtained from a precise all-electron local-density full-potential linearized-augmented-plane-wave thin-film investigation. Comparison of the theoretical photocurrent with experiment shows that only the use of these realistic surface potentials gives a proper description of surface-induced structures occurring in the experimental spectra.

Angle-resolved photoemission in the ultraviolet range has proved to be one of the most powerful methods for determining the electronic structure of a crystal. In the last few years, the determination of "experimental" band structures has become possible, allowing a direct comparison between theoretical and experimental quasiparticle properties. The so-called three-step model for the photoemission process has been widely used for the interpretation of experimental spectra as bulk bands. However, despite its apparent success in many cases, it has become very clear that the escape depth of photoelectrons excited by low-energy uv radiation is of the order of only a few angstroms. Consequently, a non-negligible amount of the spectral yield originates from the surface layer, which exhibits different electronic properties than the bulk. A rigorous theoretical description of the photoemission process embodied in a one-step model is expected to treat and account for both the bulk and the surface electronic structure on an equal footing.

In this paper we report results of the first *ab initio* calculation of the angle-resolved photocurrent using Pendry's[1,2] method and realistic surface potentials for TiC(100) obtained previously[3] using the precise full-potential linearized-augmented-plane-wave (FLAPW) method. The calculated photocurrent, when compared directly with the experimental spectra of Callenås *et al.*,[4] reveals surface-induced structures occurring in the experimental spectra which appear in the theoretical results only when realistic surface potentials are employed.

In order to make use of Pendry's[1,2] highly successful scattering formalism, the potentials in each layer of the semi-infinite crystal are taken to be of muffin-tin form by using the spherically symmetric part of the FLAPW potentials around the atoms and a planar average outside the so-called atomic spheres. While this constant potential was the same everywhere in the crystal, the spherical potentials inside the top layer of atomic spheres differed from those of the other layers. The FLAPW surface- (s-) layer potential appears in our top layer, and since the FLAPW results showed very close resemblance between the $(s-1)$-layer and central- (c-) layer potentials, the FLAPW c-layer potential is used to represent all other layers of our semi-infinite crystal. No surface relaxation was taken into account and the distance between the layers was fixed at the bulk value of 2.164 Å. For the surface potential we assumed a step barrier whose height is given by the calculated work function of 4.7 eV. The barrier is positioned immediately outside the range of the top-layer potentials. This setup for the surface barrier is in accordance with the experience gained in previous photoemission studies.[5,6]

To check the accuracy of our muffin-tin procedure, we calculated a bulk LAPW energy-band structure from the c-layer FLAPW potentials, and found very close agreement with existing results[7] (e.g., our E_F is only 0.1 eV higher than that in a bulk muffin-tin APW calculation), indicating that the FLAPW c layer is essentially bulklike.

The attenuation of the hole and photoelectron wave functions is incorporated by adding constant imaginary parts to the potentials (-0.15 eV for the low-energy hole states and -1.65 eV for the high-energy electron states). As a rule of thumb, the hole dampening tends to broaden the spectral features, whereas the high-energy constant imaginary potential also governs the escape depth of the photoelectrons.

Before presenting the calculated spectra and making comparisons with experiment we need to remark on the common practice of identifying local-density eigenvalues with excitation energies. Of course, even in the exact Hohenberg-Kohn-Sham theory only the highest occupied eigenvalue bears any physical significance as the ionization energy[8] or—as in our case—the work function.[9] In actual computations, however, the local-density eigenvalues turn out to differ only by more or less a constant shift from the true excitation energies,[10] thus leaving the band dispersions nearly unaffected. Figures 1 and 2 show the calculated spectra of the TiC(100) surface for unpolarized Ne I (16.85 eV) and He I (21.2 eV) radiation impinging along the (011) azimuth. (Both the angle of incidence of the light θ_i and

 ©1985 The American Physical Society

the electron emission angle θ_e are measured with respect to the surface normal.) The calculated spectra are therefore directly comparable to the experimental spectra displayed in Figs. 3 and 5 of Callenås *et al.*[4] Note that the theoretical spectra terminate stepwise at E_F, whereas this feature is broadened in experiment due to the finite resolution of the spectrometer. We also need to stress a small difference between the experimental and the theoretical setup concerning the angle of incidence of the uv light: The smaller theoretical θ_i of 30° as compared to the experimental 45° mimics in a simple manner the refraction occurring at the vacuum-solid interface.

One notices in Fig. 1 two different features for both $\theta_i = 30°$ and 15°, namely, one peak around −3 eV and a second peak starting just below E_F and shifting towards lower energies with increasing θ_e. At normal emission these peaks are calculated to be at −3.3 and −0.3 eV, respectively, as compared to the experimentally found values of −4.05 and −0.7 eV. These differences in the absolute peak location are not totally unexpected considering the above-mentioned inequivalence between local-density eigenvalues and the true excitation energies. The intensity of the peak at −3.3 eV is enhanced on increasing θ_i, which proves that this particular peak is sensitive to a change of the z component of the electromagnetic field. In agreement with experiment, this peak is identified as arising from bulklike carbon p states of Δ_1 symmetry. Upon moving off normal incidence, almost no dispersion is seen and the peak dies out

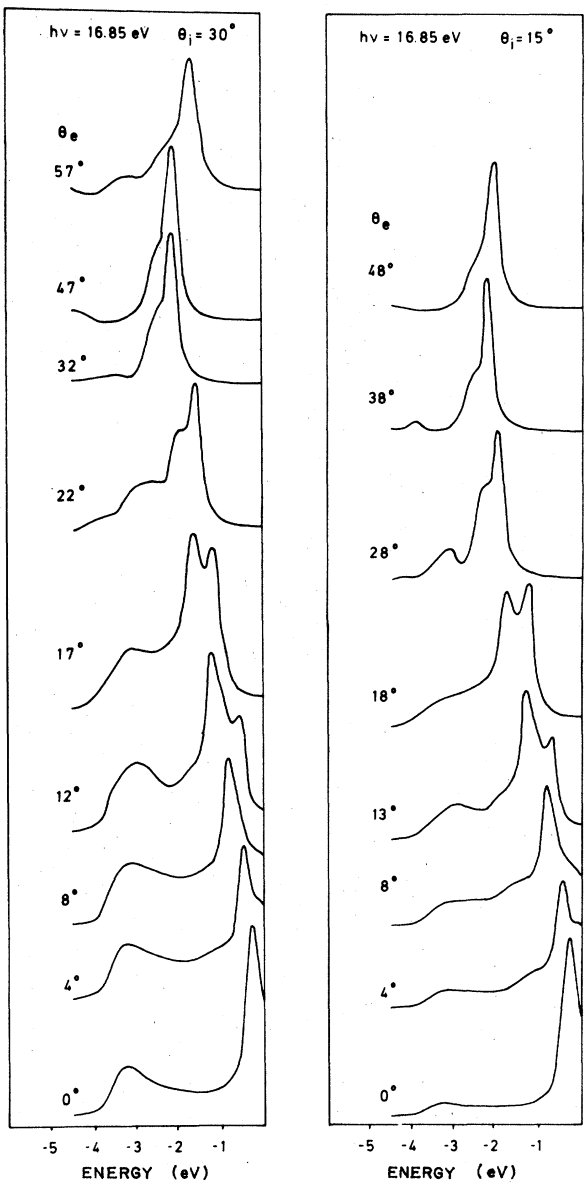

FIG. 1. Calculated angle-resolved Ne I photoemission spectra for TiC(100) along the (011) azimuth. θ_i and θ_e denote the angle of the incident photons and emitted photoelectrons with respect to the surface normal, respectively.

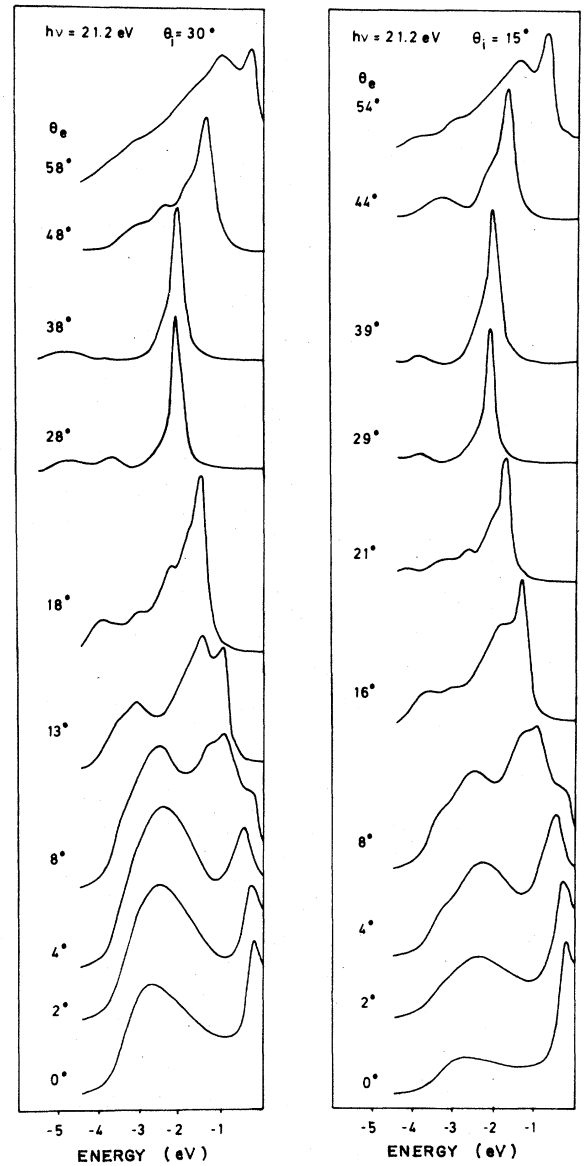

FIG. 2. Calculated angle-resolved He I photoemission spectra for TiC(100) along the (011) azimuth. θ_i and θ_e denote the angle of the incident photons and emitted photoelectrons with respect to the surface normal, respectively.

for higher emission angles. With respect to its dispersion, this peak behaves differently for He I radiation. For normal emission, Fig. 2 shows a rather broad bump centered at −2.8 eV, while experiment gives −3.5 eV. However, the relative shift from Ne I and He I (0.5 eV) proves to be correct, and so does the dispersion. Away from normal emission, this peak first shifts by 0.3 eV closer to E_F (which can be seen best for $\theta_i = 30°$), reverses its slope at about $\theta_e = 8°$, and starts moving downwards in energy very rapidly, thus following the experimentally found dispersion. In the experimental spectra for $\theta_i = 15°$ and small θ_e there is a second peak present about 1 eV higher in energy (peak C in Fig. 3 of Callenås *et al.*[2]). A closer inspection of our calculated spectra reveals that the center of this broad peak is at higher energies for $\theta_i = 5°$ than for $\theta_i = 30°$, and concomitantly a low-energy shoulder appears. This unexpected behavior suggests that this part of the spectra consists of two contributions whereby the lowest-energy contribution is diminished for smaller θ_i, thus showing the same polarization dependence as the peak in the Ne I spectra. This is in perfect agreement with the experiment. In contrast to the measured spectra, however, this two-peak structure is not entirely resolved in our calculation.

Returning to Fig. 1, we inspect in detail the peak below E_F. From the polarization dependence at normal emission we can assign this peak to an emission from bulklike carbon $p\ \Delta_5$ states. As we move away from normal, two additional structures appear, most clearly seen for $\theta_i = 15°$. Both features show up in the corresponding experimental data (peaks C and A in Fig. 5 of Callenås *et al.*[4]) The shoulder at lower energies is separated by 0.65 eV from the dominant structure, as compared to the experimentally determined energy difference of 0.6 eV. The high-energy shoulder is most pronounced for $\theta_e = 4°$ and gets weaker at higher emission angles. However, a new peak emerges at $\theta_e = 13°$ and at $\theta_e = 18°$ outgrows the former dominant structure. A similar situation is encountered for the $\theta_i = 30°$ spectra. In contrast to the Ne I spectra, the He I spectra (cf. Fig. 2) seem to lack a low-energy shoulder, both in theory and experiment. Still, the high-energy shoulder exists and is most pronounced for $\theta_e = 2°$ and loses intensity as one proceeds to $\theta_e = 4°$. At $\theta_e = 8°$, however, there is an onset of a strong new emission peak, growing rapidly with θ_e, which finally dominates the high-angle spectra, just as in the case of the Ne I radiation.

Before discussing the agreement between the theoretical and experimental dispersion and the relative intensity of this double-peak structure, it is necessary to understand the origin of this strong new feature. Figure 3 displays the unpolarized Ne I spectra of TiC(100) for $\theta_i = 15°$ and $\theta_e = 18°$ as calculated from different potentials. Our standard reference is the result obtained using the true muffin-tin FLAPW potential, denoted by FLAPW($s+c$) and an imaginary high-energy potential $\Sigma_2 = -1.63$ eV. The double-peak structure found experimentally is also found theoretically for this realistic surface potential. If one omits the surface-layer potential and uses the bulk potential also in the top layer, as shown in panel (c) denoted by FLAPW(c), this additional structure vanishes completely. That the disappearance of the double-peak structure is entirely a consequence of using only bulk potentials can also be seen from the calculation denoted by APW [panel (b)], where a self-consistent bulk APW (Ref. 7) potential was employed. In order to regain the double-peak structure one has to shift the potential at the carbon site in the top layer by about 0.4 eV. This calculation is termed APW($s = c + 0.4$ eV). A layer-by-layer decomposition of the photocurrent for our reference calculation unambigously shows that the two peaks originate from different layers. The high-energy contribution stems almost completely from the top layer, whereas the low-energy structure has a large contribution from the second layer. It is interesting to note that contributions from all other layers are completely negligible. As shown in panel (d) of Fig. 3, the contribution of the second layer can easily be enhanced by increasing the escape depth of the photoelectrons by reducing Σ_2 to −0.95 eV.

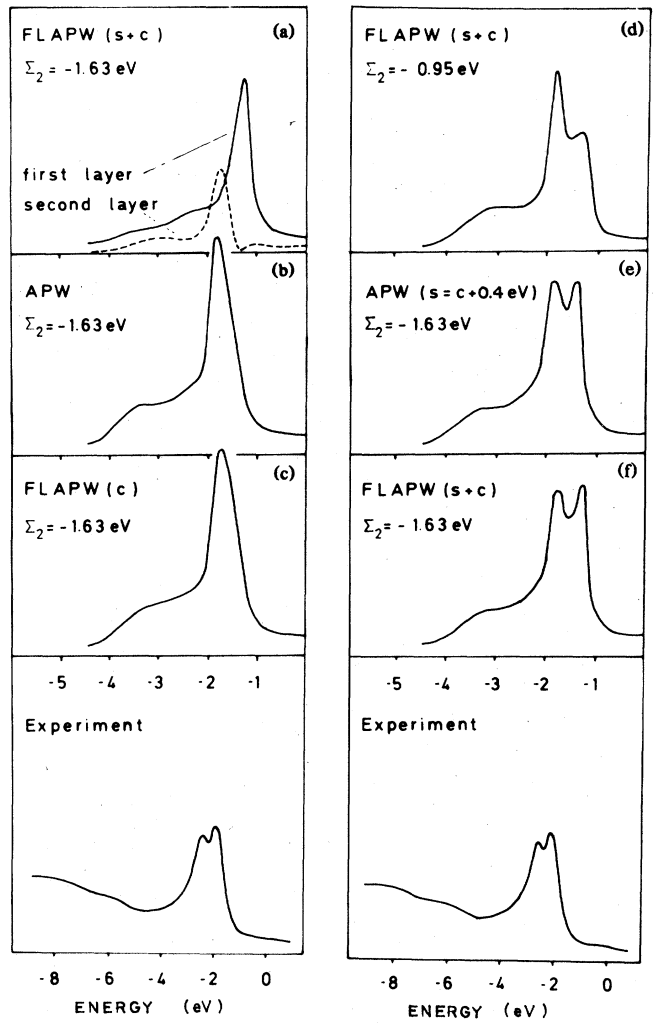

FIG. 3. Comparison with experiment of various calculated Ne I angle-resolved photoelectron spectra of TiC(100) along the (011) azimuth for $\theta_i = 15°$ and $\theta_e = 18°$ (cf. text); $h_\nu = 16.85$ eV.

The results shown in Fig. 3 clearly demonstrate the need for an accurate description of the electronic structure of the TiC surface based on realistic surface potentials such as those generated by the FLAPW method. It seems therefore necessary to be very specific about surface potentials as obtained by shifting bulk potentials by a constant as was recently done for TiC(111) (Ref. 11) and TiN(100).[5] Although the results are quite convincing, a surface-layer po-

tential shifted by a constant for TiC is not consistent with the fact that a C 1*s* core-level shift was not found in the FLAPW calculation. Of course, the more severe problem in any analysis is how to guess the magnitude of such a shift, if theoretical spectra are considered to be independent of experimentally obtained parameters.

From Figs. 1 and 2 one can see that the dispersion is reproduced theoretically quite accurately, whereas the absolute locations are misplaced by about 0.4 eV. For Ne I there are even larger deviations at $\theta_e = 13°$, 18°, 22°, 47°, and 48°. Looking at the two-dimensional FLAPW band structure shown in Fig. 4 of Wimmer, Neckel, and Freeman[3] we can easily identify the high-energy structure with states of $\bar{\Delta}_2$ symmetry dispersing towards lower energies and $\bar{\Gamma}$, or equivalently from normal emission. The agreement between calculated and experimental intensity ratios is less satisfying. The surface-layer contribution is overestimated and the peak width is too small as compared with experiment. A similar discrepancy[5] has been encountered for TiN(100) and was attributed to the distribution of the electromagnetic field inside the crystal. As can be seen from Fig. 3 the intensity ratio depends on the escape depth of the photoelectrons, which varies with emission angle. Part of the discrepancy between theory and experiment could therefore be an improper description of the angle dependence of the escape depth. Yet another possibility affecting the relative intensities could be due to the occurrence of vacancies at the carbon sites, since the experiment was actually performed on a $TiC_{0.93}$ single crystal. It has been shown recently that these vacancies also persist at the surface.[12]

Apart from these differences, the overall agreement between the experimental angle-resolved photoemission spectra and the theoretical spectra calculated from first-principles FLAPW surface potentials is very good. Furthermore, we have demonstrated that due to the small probing depth of the uv-excited photoelectrons, the use of realistic surface potentials is of crucial importance, even for the qualitative understanding of the experimental data on the TiC(100) surface.

Work at Northwestern University was supported by the National Science Foundation Division of Materials Research under Grant No. 82-16972 and the Austrian Fonds zur Förderung der Wissenschaftlichen Forschung.

[1]J. F. L. Hopkinson, J. B. Pendry, and D. J. Titterington, Comput. Phys. Commun. **19**, 69 (1980).

[2]C. G. Larsson, Ph.D. thesis, Chalmers University of Technology, Gothenburg, 1982 (ISBN 91-7032-078-0).

[3]E. Wimmer, A. Neckel, and A. J. Freeman, Phys. Rev. B **31**, 2370 (1985).

[4]A. Callenås, L. I. Johansson, A. N. Christensen, K. Schwarz, and J. Redinger, Phys. Rev. B **27**, 5934 (1983).

[5]L. I. Johansson, C. G. Larsson, and A. Callenås, J. Phys. F **14**, 1761 (1984).

[6]P. J. Durham, R. G. Jordon, and L. T. Willie, Phys. Rev. Lett. **53**, 2038 (1984).

[7]A. Neckel, P. Rastl, R. Eibler, P. Weinberger, and K. Schwarz, J. Phys. C **9**, 579 (1976).

[8]C.-O. Almbladh and U. von Barth, Phys. Rev. B **31**, 3231 (1985).

[9]N. D. Lang, in *Theory of the Inhomogeneous Electron Gas,* edited by S. Lundqvist and N. H. March (Plenum, New York, 1983).

[10]J. P. Perdew and M. R. Norman, Phys. Rev. B **26**, 5445 (1982).

[11]C. G. Larsson, J. B. Pendry, and L. I. Johansson (unpublished).

[12]M. Aono, Y. Hou, R. Souda, C. Oshima, S. Otani, and Y. Ishizawa, Phys. Rev. Lett. **50**, 1293 (1983).